Delft University of Technology

Vertical axis wind turbine wake steering by pitched struts and blades

Pinto Ribeiro, A.; Ferreira, Carlos; Casalino, D.

Important note
To cite this publication, please use the final published version (if applicable).
Please check the document version above.

PURPOSE-LED
PUBLISHING™

PAPER • OPEN ACCESS

Vertical axis wind turbine wake steering by pitched struts and blades

View the article online for updates and enhancements.

Vertical axis wind turbine wake steering by pitched struts and blades

André F. P. Ribeiro, Carlos S. Ferreira, and Damiano Casalino

Delft University of Technology, Delft, the Netherlands

E-mail: `a.pintoribeiro@tudelft.nl`

Abstract. Vertical axis wind turbines (VAWTs) have been identified as a technology that, in association with wake steering, can increase power density of wind farms. In this study, we validate a free wake method for VAWT wake prediction, which leads to satisfactory results. We then use this method to simulate wake steering by means of fixed pitched blades and struts. We demonstrate that combining pitched wakes and struts can lead to very advantageous wake behavior, but only when the interactions between the tip vortices are taken into account. The possibility to inject more high momentum flow into the wake while moving the vortex system away from the next turbine could make pitched blades and struts a powerful tool for future wind farms.

1. Introduction

With the recent global shift towards renewable energy, the interest in wind energy is growing every year. Traditional horizontal axis wind turbines have been the preferred method for extracting energy from the wind. However, interest in vertical axis wind turbines (VAWTs) is on the rise, due to their advantages over traditional turbines. The main benefits of VAWTs are: the fact that the generator can be at ground level, leading to easier installation and maintenance; noise reduction, due to lower tip speeds; and the omnidirectional wind capture without the need for a yawing mechanism.

As onshore and offshore wind farms become larger, reducing the distance between the turbines without substantial loss to the power production of each turbine is an important research and industrial topic, as the interaction between the wakes becomes a critical phenomenon. Many research groups have investigated wake steering and other forms of control in order to increase the power densities of future wind farms [1]. Recent studies have investigated the effects of static and dynamic VAWT blades pitching [2], which besides potentially improving power production [3, 4, 5], can also be used to improve wake recovery [6]. Improving wake recovery with fixed blade pitching usually comes with a performance penalty on the first turbine and a performance gain on the downstream turbines. A study on the aerodynamic effects of the horizontal supports holding the blades (struts) has also shown promising results [7]. Fixed pitched struts could be structurally advantageous, as the moment of inertia around the horizontal axis is increased when using airfoil shaped struts. To the authors' knowledge, the combination of pitching blades and struts has not yet been investigated.

In this work, we perform numerical simulations of pitched VAWTs using a free wake panel method, which are validated with computational fluid dynamics (CFD) simulations performed by Ming [6], who used actuator line unsteady Reynolds-averaged Navier-Stokes (URANS), with the $k-\epsilon$ turbulence model. The free wake simulations allow us to examine the unsteady interaction of the vortices created by blade and strut pitching in a cost-effective manner. As

the wake steering effects from pitching are dominated by advection effects (instead of diffusion or mixing effects) in the near-wake, Lagrangian methods are a promising approach to examine potential benefits from pitching. We then go beyond the previous studies and include pitched struts along with the pitched blades. The objectives of this work are to validate the free wake panel method for VAWT wake steering and to verify the potential gains in wake steering from combined pitching of blades and struts.

2. Methods

We employ a source and doublet panel method with free wake modelling [8]. The code employed in this work was recently validated for moving airfoils and wind turbine rotors [9], including several dynamic effects [10] and flexible wing aeroelasticity [11]. The thickness effects are fully captured, as the triangular or quadrilateral panels lie on the blade surfaces. The method uses a boundary element approach, with each surface panel and wake filament influencing all the others [12], meaning no volume mesh is needed. The surface and wake discretizations of the velocity potential equation lead to the following:

$$\frac{1}{4\pi}A_{ij}\mu_j + \frac{1}{4\pi}B_{ij}\sigma_j + \frac{1}{4\pi}C_{iw}\gamma_w = 0, \tag{1}$$

where A_{ij}, B_{ij}, and C_{ij} are the influence coefficients matrices [12] for the doublets μ, sources σ, and wake vortices γ respectively. This equation corresponds to the different contributions to the flow potential on the center a surface panel i, where there are contributions from all surface panels j and all wake panels w. The values of μ, σ, and γ are constant over each panel.

The sources σ are computed to ensure impermeability, while vortex strength γ of the first row of wake panels is enforced with the Kutta condition [13]. These values of γ are then convected over time as new wake panels are created at the trailing edge at each timestep. The influence coefficients in Eq. 1 can then be computed by solving the linear system.

Traditional free wake panel methods have issues with singularities when wakes intersect solid bodies. This happens due to divisions by zero in the equations for the influence coefficients. One way to avoid this issue is by switching the formulation of the wake panels from velocity potential to velocity panels [14] after a certain row of wake panels. Changing the wake formulation to the far wake, the singularities in C_{iw} are replaced with singularities in the Biot-Savart law. These can be then avoided by using a vortex core model [15], thus stabilizing the problem and allowing for wake-blade interaction. The velocities induced on the body by the far wake must be accounted for in σ and in the unsteady Bernoulli equation [16]. More details about the mathematical formulation of the method and the validation of our implementation can be found in [17].

For a horizontal wind turbine operating at zero yaw and tilt, and operating under constant freestream velocity, σ is constant for each panel throughout the simulation, as the far wake formulation is not needed and the remaining vectors remain at constant values and relative angles. For VAWTs, σ changes at every timestep, as the angle between the freestream velocity $\vec{U}_\infty$ and the other vectors (kinematic velocity and surface normal vectors) change. Additionally, the velocity induced by the far wake on the surface also changes over time. In early resolution studies, we noticed this case was more sensitive to the timestep than previous simulations and realized the calculation of the kinematic velocity of each surface panel $\vec{u}_{body}$ was the reason, as using a first order backward Euler finite difference approach was inaccurate. We hence use a second order approach in this work, which solved this issue.

Symmetry conditions can be used in the code by means of virtual panels. Although VAWTs are not aerodynamically axisymmetric, the VAWTs in this work have symmetry over

the horizontal plane, which can be exploited to reduce the influence coefficient matrices from $N \times N$ to $N/2 \times N/2$, where N is the number of surface panels. Also, the number of wake panels that need to be computed is halved, although the number of Biot-Savart computations on a given point is the same, but using virtual panels.

3. Case Description

In this work, we simulate the three-bladed VAWT that was used in the work of [6]. This is a high Reynolds VAWT, which is more suitable for the inviscid method used in this work than small scale VAWTs. A sketch of the top and side view of the VAWT is given in Fig. 1. The freestream velocity U_∞ is 10 m/s, the tip speed ratio $\lambda = \Omega R/U_\infty$ is set to 4.5, where Ω is the angular velocity, and R is the turbine radius. This condition was chosen as it is near the maximum power coefficient for this turbine. The VAWT is square in cross section, meaning the height H is equal to the diameter D, which is 160 m. The blades have chord $c = D/40$ and can have zero pitch angle, or $\pm 10°$, where a positive pitch means the nose points towards the center of the rotor. Struts are included in some of the simulations, which was not the case in the reference results. They are lifting surfaces with the same chord as the blades, with a starting radius of $0.13R$ and a maximum radius of $0.99R$. The struts can have the same pitch angle as the blades, where a positive pitch means the nose pointing away from the turbine horizontal symmetry plane. The blades and struts have NACA0025 cross sections.

For the discretization of the blades and struts, we use 50 panels over the blades height and 22 panels over the struts span, with homogeneous spacing. For the blades and struts we use 200 panels around the chordwise direction, with cosine spacing, i.e. refinement on the leading and trailing-edges. The timestep corresponds to 6° rotation of the turbine and simulations are run for at least 960 timesteps, i.e. 16 full rotations or over 11 flow passes over the rotor diameter. The simulated geometry, in correct proportions, is shown in Fig. 2.
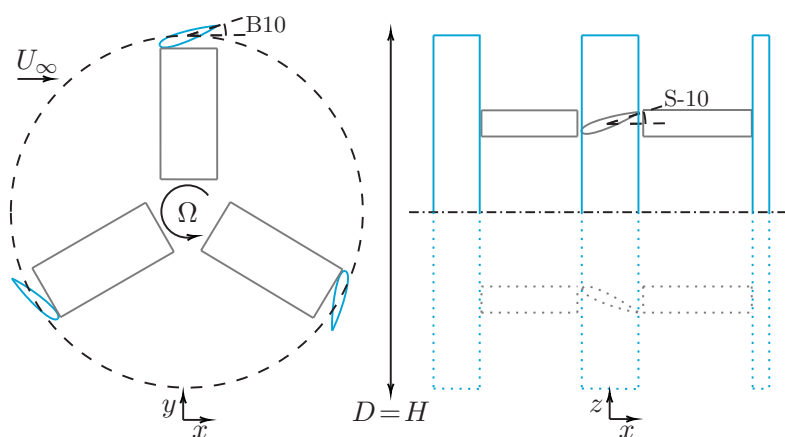
Figure 1: Sketch of the VAWT. Not to scale. Top view on the left, side view on the right. Symmetry plane shown as dash-dotted line. Blade path shown as dashed circle. Virtual panels shown in dotted lines. Positive blade pitch and negative strut pitch illustrated. Blades are in blue, struts in grey.

Early simulations with small values for the radius used in the vortex core model had very unstable wakes. Previous experience with this method [10] has shown that in order for complex wakes to be preserved, large values of the core radius are needed. We hence set the radius to about twice the chord of the blades and struts (or about $D/20$). This allowed us to preserve

Figure 2: Top half of the VAWT as simulated in this work. To scale. Blades and struts are pitched as in Fig. 1.

the wakes of the VAWTs while still obtaining reasonable values for the power coefficients when compared to reference CFD.

The nomenclature used throughout this paper describes cases based on the blade pitch angle and strut pitch angle. Cases with no struts and blades pitched at -10, 0, and 10° are named B-10, B0, and B10 respectively. Cases with the struts pitched at -10, 0, and 10° are named S-10, S0, and S10 respectively. Hence, the case in Fig. 1 is referred to as B10S-10.

4. Results

4.1. Validation of single turbine with pitched blades and no struts

We begin by comparing results from our simulations with reference CFD results [6]. Figure 3 shows the wakes of each of the three cases simulated in this section, along with the measurement planes at $x = 1D$, $3D$, and $5D$, which will be used for comparisons to reference data. Blade pitching clearly has strong wake steering effects, with positive pitching contracting the wake axially and spreading it laterally, while negative pitching (as we will see later) has the opposite effect. B0 is the only case where the wake is nearly symmetric, as the other cases have asymmetric vortices appearing at the corners of the turbine, which are responsible for the wake steering [18].

Figure 4 shows planes perpendicular to the streamwise direction, where the bottom halves of the nine squares show CFD data, while the top halves are the panel code results. The planes show time-averaged streamwise velocity u normalized by the freestream velocity. The grey squares at the center of the images are the outline of the VAWTs. The CFD and free wake results use similar resolutions in the planes, but the free wake vectors were drawn at lower density for clarity. Near the turbine, at $x = 1D$, results are very similar between both methods. Discrepancies increase at $x = 3D$, while at $x = 5D$ the results become quite different. Free wakes made of vortex filaments tend to become entangled over long distances and this leads to large errors. In addition, for all figures the CFD results show more diffusion of the wake than panel code results. This is expected, as CFD tends to cause too much dissipation and diffusion, while Lagrangian methods tend to have too little of both. In spite of such differences, the wake steering from the pitched blades is captured and the shapes of the wakes are very similar.

Throughout the work we use the power coefficient C_P to measure the effects of pitching

(a) B-10.   (b) B0.   (c) B10.
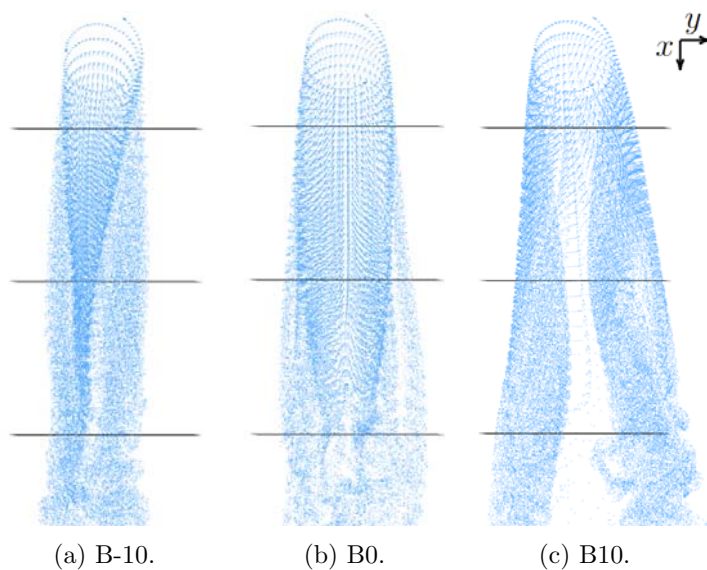
Figure 3: Top view of wakes generated by each blade pitch setting. Horizontal lines are the planes at $x = 1D$, $3D$, and $5D$, from top to bottom, where $x = 0$ is at the rotor axis.
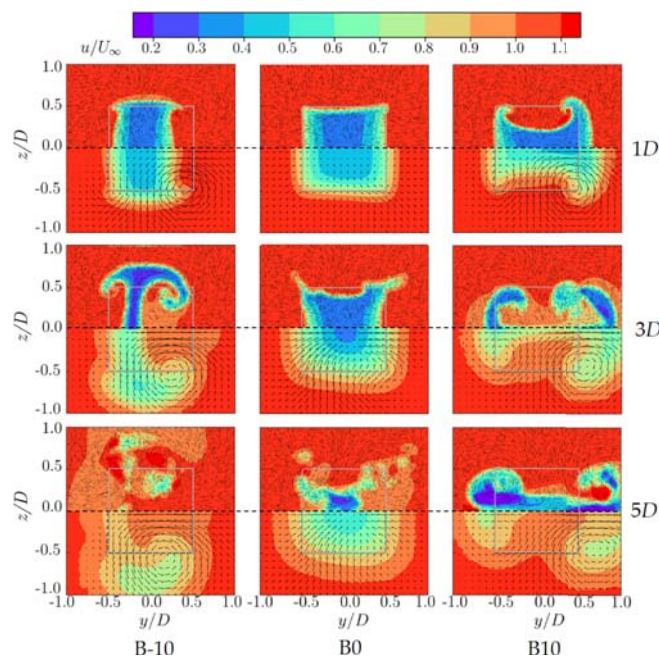
Figure 4: Planes perpendicular to the streamwise direction. The rows are, from top to bottom, $1D$, $3D$, and $5D$ downstream of the VAWT center. The columns correspond to different blade pitch angles. The top half of each square corresponds to free wake results, while the bottom halves are the reference CFD [6].

on the turbine power production. It can be computed as:

$$C_P = \Omega Q / (0.5 \rho U_\infty^3 DH), \tag{2}$$

where Q is the turbine torque and ρ the air density. Table 1 shows the effect of blade pitching on C_P for the current simulations and the reference CFD. The inviscid methods used in this

work have limitations in calculating C_P accurately [9], as the torque requires sectional drag to be accurate. Hence, we do not expect a perfect match. With viscous drag being neglected, the power calculated with the panel code is higher than in CFD. The losses due to blade pitching are also higher than the reference, but the qualitative agreement is fair, with both methods predicting B10 to have the worst performance, then B-10, and then B0. These results give some confidence to the method, but also serve as a warning that the effects of pitching obtained for the remainder of the paper are potentially overpredicted.

Table 1: Power coefficient for the VAWTs. Current results compared to the reference CFD. Values in red indicate the loss of power relative to B0 of the corresponding method.

	B-10	B0	B10
Panel Code	0.50 (-11%)	0.56	0.48 (-14%)
CFD [6]	0.46 (-8%)	0.50	0.44 (-12%)

As expected, pitching the blades leads to lower power for the VAWT. The expected benefit of blade pitching is in wake steering, trying to improve the power of the downstream turbines in a manner that compensates the power loss for the upstream turbine. The power available for the downstream turbine can be estimated by computing the average of u^3/U_∞^3 on a downstream plane the size of the frontal area of a potential downstream turbine. In a case with optimal wake steering, where the wake is moved completely outside of the grey squares representing the turbine outlines (which also represent the position of potential downstream turbines) in Fig. 4, this available power would be one. When the wake does not spread outside of the location of the downstream rotors, the available power is low. Streamwise vortices can energize the wake by advecting high speed flow from the surrounding area into the downstream rotor locations.

For completeness, we also examine the streamwise (x) and lateral (y) thrust coefficients for these cases:

$$C_{Tx|y} = F_{x|y}/(0.5\rho U_\infty^2 DH),\tag{3}$$

where F is the force acting on the rotor and $x|y$ represents that the force and corresponding coefficient can be taken in the x or y directions. Results for C_T are shown in Table 2. While the lateral thrust is in fair agreement with the CFD, the streamwise thrust is substantially overpredicted. This is not surprising given the very high angles of attack found in the flow conditions studied here, which can potentially lead to inaccuracies due to excess flow separation in CFD and certainly cause inaccuracies in the inviscid panel method, which has no flow separations. Hence, these results highlight some of the limitations of the method employed in this work.

Table 2: Thrust coefficients for the VAWTs. Current results compared to the reference CFD.

	B-10	B0	B10
C_{Tx} Panel Code	0.88	0.81	0.88
C_{Tx} CFD [6]	0.69	0.68	0.64
C_{Ty} Panel Code	-0.46	0.02	0.38
C_{Ty} CFD [6]	-0.37	0.02	0.34

The available power for potential downstream rotors at $x=3D$ is shown in Table 3. The differences between CFD and panel code in available power for B0 is far larger than for B-10 and B10, since the wake at B0 is diffusion dominated, while the other case have strong advection effects. As mentioned before, diffusion is likely overestimated in the CFD results and certainly underestimated in the free wake results. Other potential sources of differences are the interactions between the vortices, as the free wake simulations do not account for merging and breakup of the vortical structures.

Table 3: Power available for a VAWT at $x=3D$. Blue values in parentheses indicate gain over B0 for the respective method.

	B-10	B0	B10
Panel Code	0.63 (5.9×)	0.11	0.61 (5.7×)
CFD [6]	0.64 (2.6×)	0.25	0.72 (2.9×)

4.2. Validation of two turbines with pitched blades and not struts

We now investigate an array of two turbines: the first with pitched blades and the second, placed at $x=3D$, without blade pitching (B0). This was also simulated in [6] and here serves to validate the use of free wake panel methods for VAWT wake interaction. The time histories of C_P for the three cases are shown in Fig. 5. Whereas integrating the available power in the wake of B0 led to substantial differences between free wake and CFD simulations (see Table 3), the agreement of simulating two turbines is very good. This could be due to the presence of the downstream turbine creating more local advection effects, that compensate for the errors in diffusion. For the three cases we can observe reasonably good agreement, but also very slow convergence. This is because the wake of the first turbine needs to travel a distance of $3D$, then interact with the second turbine, and then propagate further to remove the startup vortex effects from both turbines.

(a) B-10.   (b) B0.   (c) B10.
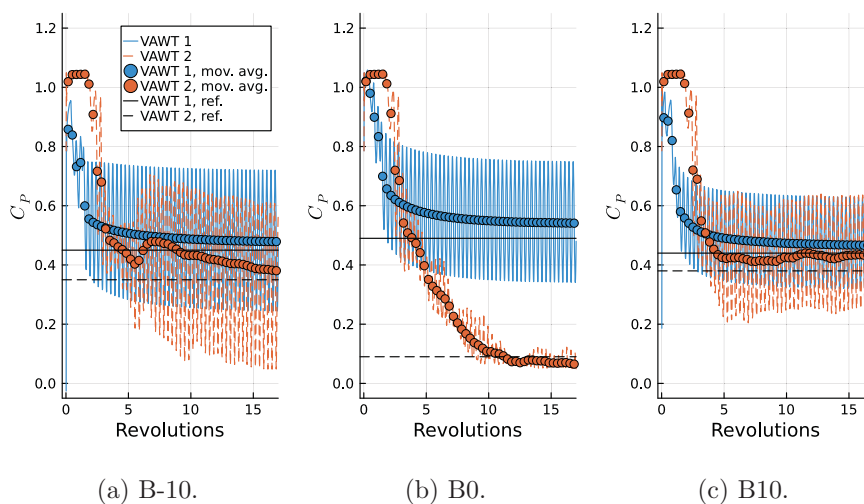
Figure 5: Time history of the power coefficient for the two turbine arrays. Reference results are CFD from [6].

Top and side views of the three simulations are shown in Fig. 6. As soon as the wakes reach the second turbine, they become extremely tangled and the flow downstream of that
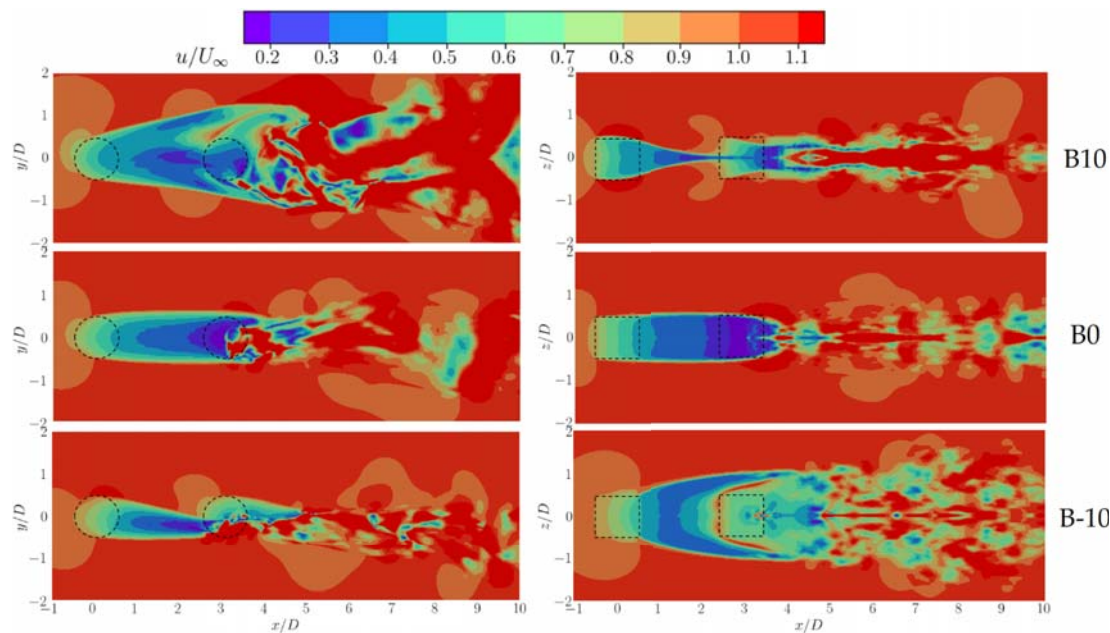
Figure 6: Top (left) and side (right) views of the turbine pairs. The downstream turbine is always B0 and is at $x = 3D$.

region is not meaningful, which indicates that even if the current free wake simulations are fast and accurate enough compared to the CFD, adding another downstream turbine is unfeasible.

4.3. Combining blade and strut pitching

We now investigate the effects of including and pitching the struts of the blades. The top and bottom struts are always pitched in opposite directions, making the case symmetric around the $z = 0$ plane. The power coefficient C_P for all cases is shown in Table 4. Comparing these results with Table 1, we can see that adding the struts at zero pitch has a small effect of about 2% on C_P. Blade or strut pitching seems to decrease C_P by nearly 10%, with the exception of B0S-10, which has minor effects. Combining blade and strut pitching tends to have a cumulative effect, reducing power by almost 20%, with the exception of B10S10, which has a much larger power loss.

Table 4: Power coefficient for the VAWT. Percentage decrease in power relative to B0S0 shown in red.

	B-10	B0	B10
S10	0.45 (-19%)	0.50 (-9%)	0.39 (-30%)
S0	0.51 (-8%)	0.55	0.47 (-15%)
S-10	0.45 (-19%)	0.55 (-1%)	0.48 (-14%)

The wake planes at $x = 3D$ for the nine configurations are shown in Fig. 7. The center row is similar to the center row of Fig. 4, with small differences due to the presence of the struts, even though they are at zero pitch angle. By looking at the center column, we can observe pitching the struts has similar effects to pitching the blades, with a positive pitch leading to the wake being stretched to the sides and a negative pitch pushing the wake to the top and

bottom. The four corner images show the effects of combining blade and support pitching, which seems to be favorable for B10S-10 and less effective for B-10S10. These results are not intuitive, as if blade and strut pitching tend to move the wake in the same direction, one would expect B10S10 and B-10S-10 to be the optimum cases.
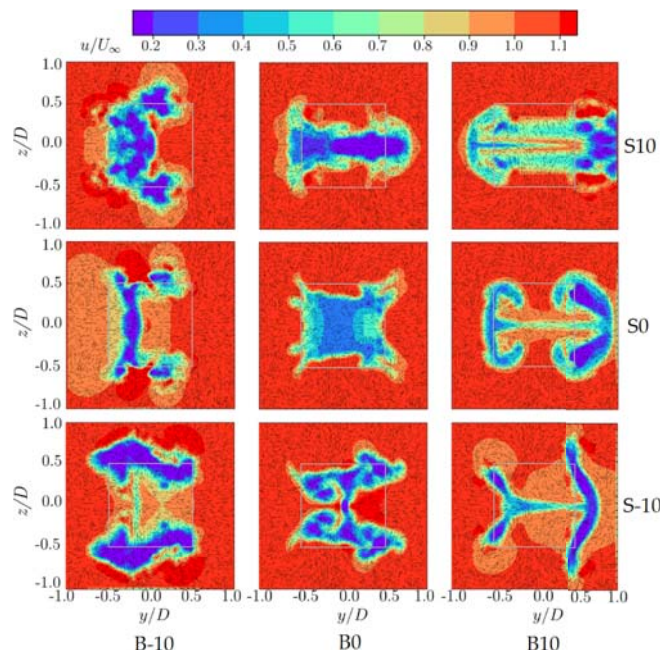
Figure 7: Planes perpendicular to the streamwise direction at $x = 3D$. The rows correspond to different horizontal supports pitch angles. The columns correspond to different blade pitch angles.

Again, we evaluate the available power in the wake of the turbines, at a distance of $3D$. This location is selected due to being close enough to avoid excessive wake entanglement, but far enough that it could potentially be used in a high-density turbine array. Results are summarized in Table 5. Given the inaccuracies seen in Section 4.1, the computed trends could be misleading, but, assuming the trends are reasonable, the gains with strut pitching are substantially lower than with blade pitching, which is consistent with the fact that the blades are longer and translate faster than the struts. However, a few cases are noteworthy: first, B0S-10 provides fair improvement over the baseline ($2.4\times$), with very little penalty to the upstream turbine (-1%), although other cases can lead to overall higher power output (sum of power for the two turbines) due to superior wake recovery. Second, B10S-10 is the only case where combined pitching is more effective than blade pitching. Finally, B-10S0 and B10S0 show that the struts at zero pitch have a noticeable effect in the downstream power, compared to the cases in Table 3.

In order to investigate the physics of the vortex system acting on the wake, we now focus on the wake filaments coming from the tips of the blades and struts in the near wake of the VAWTs. An isometric representation of what we will investigate here is shown in Fig. 8 for clarity. The actual analysis is shown in Fig. 9, which has vertical cuts of the wakes seen from donwstream of the turbines, where only the top halves of the VAWTs are shown, along with circles indicating the direction of the vorticity generated by the wake filaments. The blade wakes are blue and the strut wakes are red. We can now understand the effects of the cases of combined strut and blade pitching. Cases B-10S-10 and B10S10 theoretically should work

Table 5: Power available for a VAWT at $x = 3D$. Blue values in parentheses indicate gain over B0S0.

	B-10	B0	B10
S10	0.42 (2.9×)	0.46 (3.2×)	0.50 (3.5×)
S0	0.56 (3.9×)	0.14	0.64 (4.5×)
S-10	0.46 (3.3×)	0.35 (2.4×)	0.70 (4.9×)

well, as both the blade and struts are trying to pull high momentum flow into the wake from the same direction (the sides and the top/bottom, respectively). However, we see that in these cases the vortices created by the struts and blades are close together and spinning in the same direction, working against each other in the region between them. Case B-10S10 has counter rotating vortex pairs, but they are working to expand the wake in all directions, only pulling flow into the wake in the small region between the vortices.
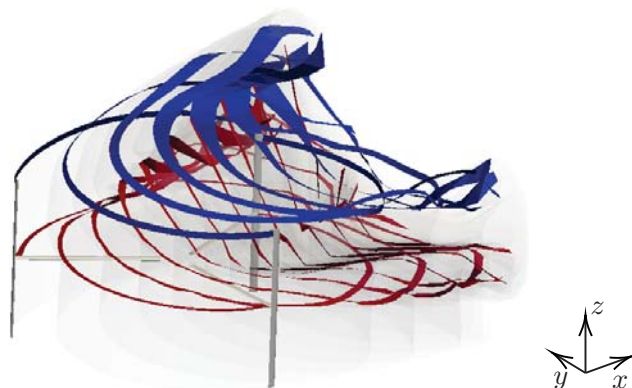
Figure 8: Isometric view of the data shown in Fig. 9. Top half of case B10S-10. The wake panels are trimmed at $x = 0.8D$ and colored in transparent grey. The blade tip vortices are shown as blue ribbons. The strut tip vortices are shown in red ribbons.

The case that works best based on previous analyses is B10S-10 and Fig. 9 clarifies the reason for this. The vortex pairs are counter rotating, working together to move the wake to the outside diagonals. They are also arranged in ways that allow them to propel themselves outwards, moving the vortex cores away from the wake, which the other cases do not achieve well, allowing for strong wake steering. Finally, the vortices are pulling high momentum flow into the wake from the sides and top/bottom, energizing the flow in a more effective way.

5. Conclusions

In this study, we have explored various VAWT configurations with pitched blades and struts in an attempt to model wake steering with a free wake panel method. The key findings from this research are:

- Simulating an isolated VAWT with a free wake panel method leads to reasonable power prediction. Estimating power available for the next turbine is limited to short distances (three diameters in our case, but increasing vortex cores can stabilize wakes further) and is inaccurate in cases that are dominated by diffusion.
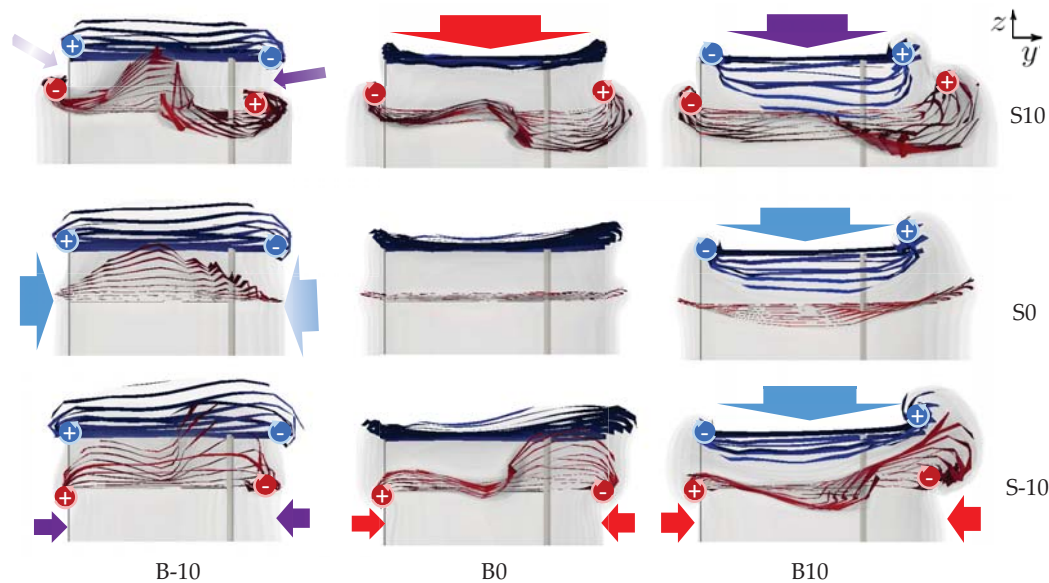
Figure 9: View towards upstream of all cases with struts. Tip wake filaments of the struts shown in red, and in blue for the blades. Remaining filaments shown in transparent grey. Positive (counter-clockwise) and negative (clockwise) vorticity regions highlighted with circles. Large arrows indicate flow being injected into the wake by the vortices, with colors indicating which vortices are inducing the airflow (red: struts, blue: blades, purple: both). Only top half of the VAWTs shown due to symmetry.

- Simulating sets of turbines downstream from each other showed good accuracy in power prediction, but is limited to two turbines, as the wakes become entangled after the second turbine. Such simulations take over a day in a desktop computer with 20 cores and a GPU with 8 GB of RAM. This time could likely be substantially reduced with acceleration techniques, such as the fast multipole method.

- For the cases studied here, strut pitching was less effective than blade pitching for wake steering. Combining strut and blade pitching can be very effective, but only if the interaction between the tip vortices are well accounted for.

The design that we investigated was symmetric around the horizontal plane, which might be necessary for good interaction between the strut and blade vortices to be achieved. Results from previous strut pitching studies investigated wake steering by pitching the upper and lower struts in the same direction [7] need to be reconsidered when combining blade and strut pitching.

While the lack of dissipation and diffusion in the current method tends to overpredict the power reduction in the wake of the turbine, combined with the fact that the inviscid approach does not include potential dynamic stall effects, the reported results reveal, for the first time, the potential of combining blade and strut pitching to achieve a higher wind-farm power density. In this respect, the present low-fidelity method can provide useful preliminary qualitative information about the vortical wake structure, but do not replace the usage of higher fidelity approaches to calculate the true benefits of blade and strut pitching in VAWTs, taking also into account wind shear, incoming turbulence from the atmospheric boundary layer, and ground effects.

References

[1] D. R. Houck, "Review of wake management techniques for wind turbines," *Wind Energy*, vol. 25, no. 2, pp. 195–220, 2022.

[2] B. LeBlanc and C. Ferreira, "Estimation of blade loads for a variable pitch vertical axis wind turbine from particle image velocimetry," *Wind Energy*, vol. 25, no. 2, pp. 313–332, 2022.

[3] M. Elkhoury, T. Kiwata, and E. Aoun, "Experimental and numerical investigation of a three-dimensional vertical-axis wind turbine with variable-pitch," *Journal of Wind Engineering and Industrial Aerodynamics*, vol. 139, pp. 111–123, 2015.

[4] B. K. Kirke and B. Paillard, "Predicted and measured performance of a vertical axis wind turbine with passive variable pitch compared to fixed pitch," *Wind Engineering*, vol. 41, no. 1, pp. 74–90, 2017.

[5] B. Chen, S. Su, I. M. Viola, and C. A. Greated, "Numerical investigation of vertical-axis tidal turbines with sinusoidal pitching blades," *Ocean Engineering*, vol. 155, pp. 75–87, 2018.

[6] M. Huang, "Wake and wind farm aerodynamics of vertical axis wind turbines," Ph.D. dissertation, Delft University of Technology, 2023.

[7] V. Mendoza and A. Goude, "Improving farm efficiency of interacting vertical-axis wind turbines through wake deflection using pitched struts," *Wind Energy*, vol. 22, no. 4, pp. 538–546, 2019.

[8] J. Katz and A. Plotkin, *Low-Speed Aerodynamics*, 2nd ed., ser. Cambridge Aerospace Series. Cambridge University Press, 2001.

[9] A. F. P. Ribeiro, D. Casalino, and F. C. S., "Surging wind turbine simulations with a free wake panel method," *Journal of Physics: Conference Series*, vol. 2265, no. 4, p. 042027, may 2022.

[10] A. F. P. Ribeiro, D. Casalino, and C. S. Ferreira, "Nonlinear inviscid aerodynamics of a wind turbine rotor in surge, sway, and yaw motions using a free-wake panel method," *Wind Energy Science*, vol. 8, no. 4, pp. 661–675, 2023.

[11] A. F. P. Ribeiro, D. Casalino, and C. Ferreira, "Free wake panel method simulations of a highly flexible wing at flutter," in *AIAA AVIATION Forum*, 2022.

[12] B. Maskew, "Program VSAERO theory document: A computer program for calculating nonlinear aerodynamic characteristics of arbitrary configurations," National Aeronautics and Space Administration, Contractor Report 4023, 1987.

[13] H. Youngren, E. Bouchard, R. Coopersmith, and L. Miranda, "Comparison of panel method formulations and its influence on the development of QUADPAN, an advanced low-order method," in *Applied Aerodynamics Conference*, 1983.

[14] M. Gennaretti and G. Bernardini, "Novel boundary integral formulation for blade-vortex interaction aerodynamics of helicopter rotors," *AIAA Journal*, vol. 45, no. 6, pp. 1169–1176, 2007.

[15] M. Ramasamy and J. G. Leishman, "A Reynolds number-based blade tip vortex model," *Journal of the American Helicopter Society*, vol. 52, no. 3, pp. 214–223, 2007.

[16] G. Bernardini, J. Serafini, M. Molica Colella, and M. Gennaretti, "Analysis of a structural-aerodynamic fully-coupled formulation for aeroelastic response of rotorcraft," *Aerospace Science and Technology*, vol. 29, no. 1, pp. 175–184, 2013.

[17] A. F. Ribeiro, C. Ferreira, and D. Casalino, "On the use of filament-based free wake panel methods for preliminary design of propeller-wing configurations," *Aerospace Science and Technology*, vol. 144, p. 108775, 2024.

[18] D. D. Tavernier, C. Ferreira, U. Paulsen, and H. Madsen, "The 3D effects of a vertical-axis wind turbine: rotor and wake induction," *Journal of Physics: Conference Series*, vol. 1618, no. 5, p. 052040, sep 2020.